Supporting Information:

Integrating Chemical Engineering and Crystallographic Texturing Design Strategy for Realization of Practically Viable Lead-Free Sodium Bismuth Titanate-Based Incipient Piezoceramics

Wangfeng Bai*,†, Xinyu Zhao†, Yanwei Huang§, Yuqin Ding†, Leijie Wang†, Peng Zheng*,†, Peng Li‡, Jiwei Zhai*,⊥

† College of Materials and Environmental Engineering, Hangzhou Dianzi University, Hangzhou, 310018, China

‡ College of Materials Science and Engineering, Liaocheng University, Liaocheng, 252059, China

§ State Key Laboratory of Precision Spectroscopy, East China Normal University, Shanghai, 200062 China

⊥Functional Materials Research Laboratory, School of Materials Science & Engineering, Tongji University, No. 4800 Caoan Highway, Shanghai 201804, China

***Corresponding authors:**

*E-mail address: bwfcxj@126.com (W. Bai)

*E-mail address: zhengpeng@hdu.edu.cn (P. Zheng)

*E-mail address: apzhai@tongji.edu.cn (J. Zhai)

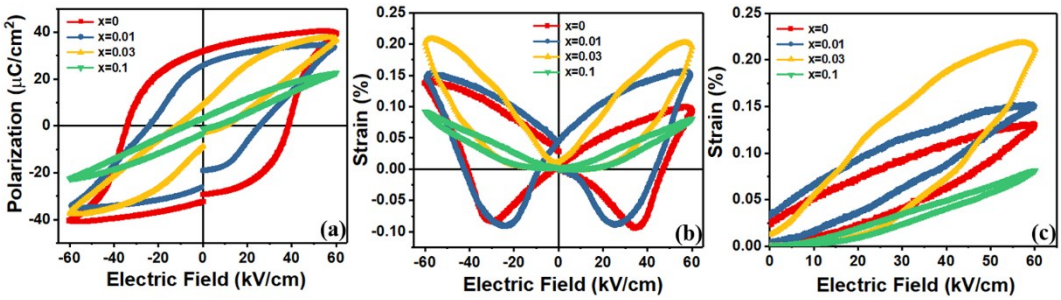

Figure S1. (a) Polarization hysteresis, (b) bipolar strain, and (c) unipolar strain loops for the BNT-BT-NN ceramics with different NN content prepared by CSSR method.

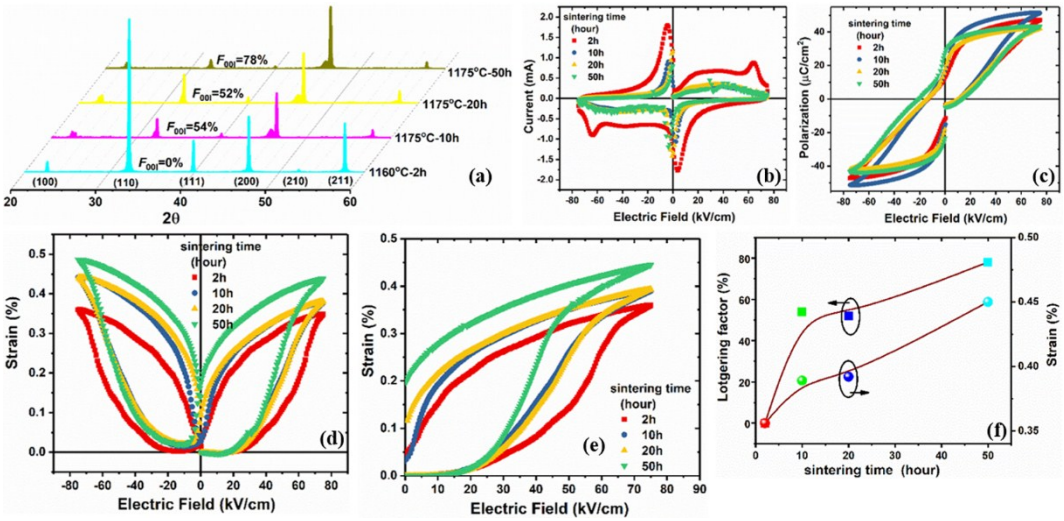

Figure S2. (a) XRD patterns, (b) field-current curves, (c) polarization hysteresis loops, (d) bipolar strain curves, (e) unipolar strain curves, and (f) strain values and Lotgering factor of BNT-BT-NN ceramics with respect to sintering time.

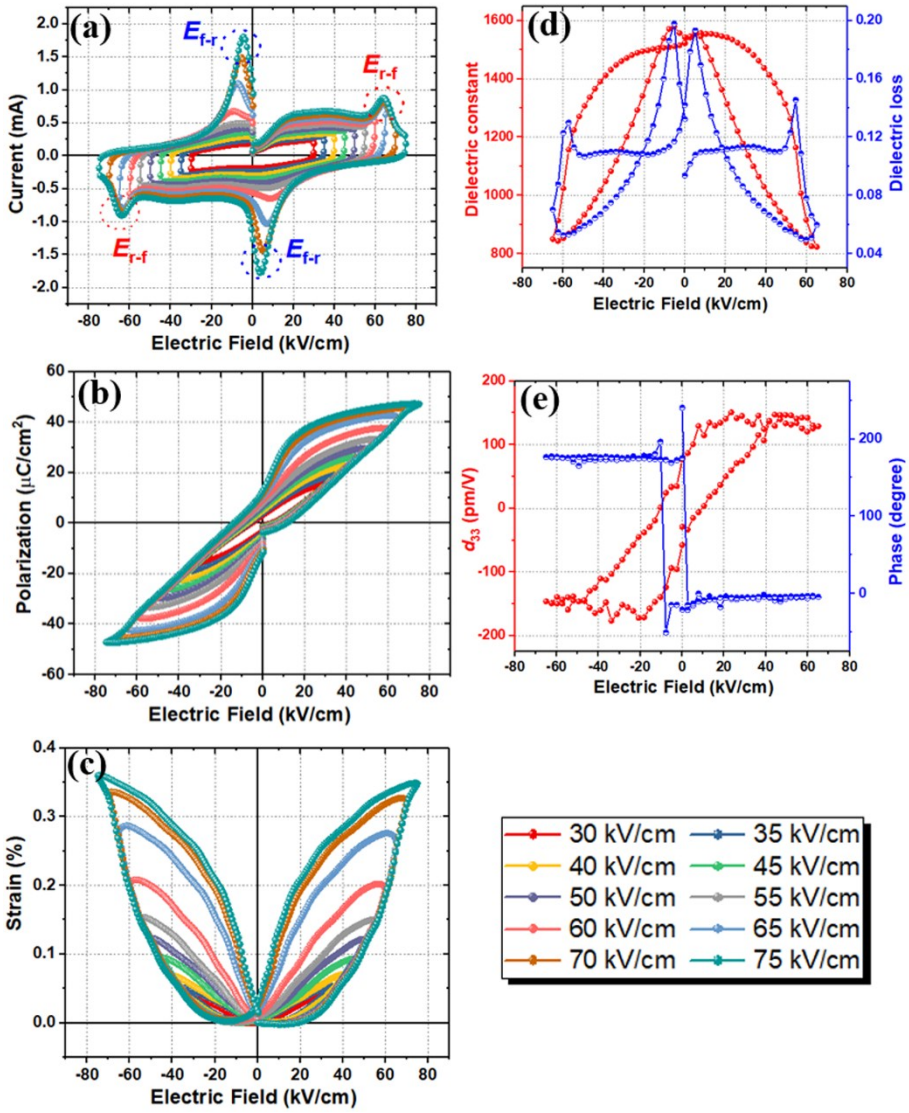

Figure S3. Electric field-dependent (a) current-field curves, (b) polarization hysteresis loops, (c) bipolar strain curves, (d) dielectric constant and loss, and (e) piezoelectric strain coefficient and phase curves for the random ceramics.

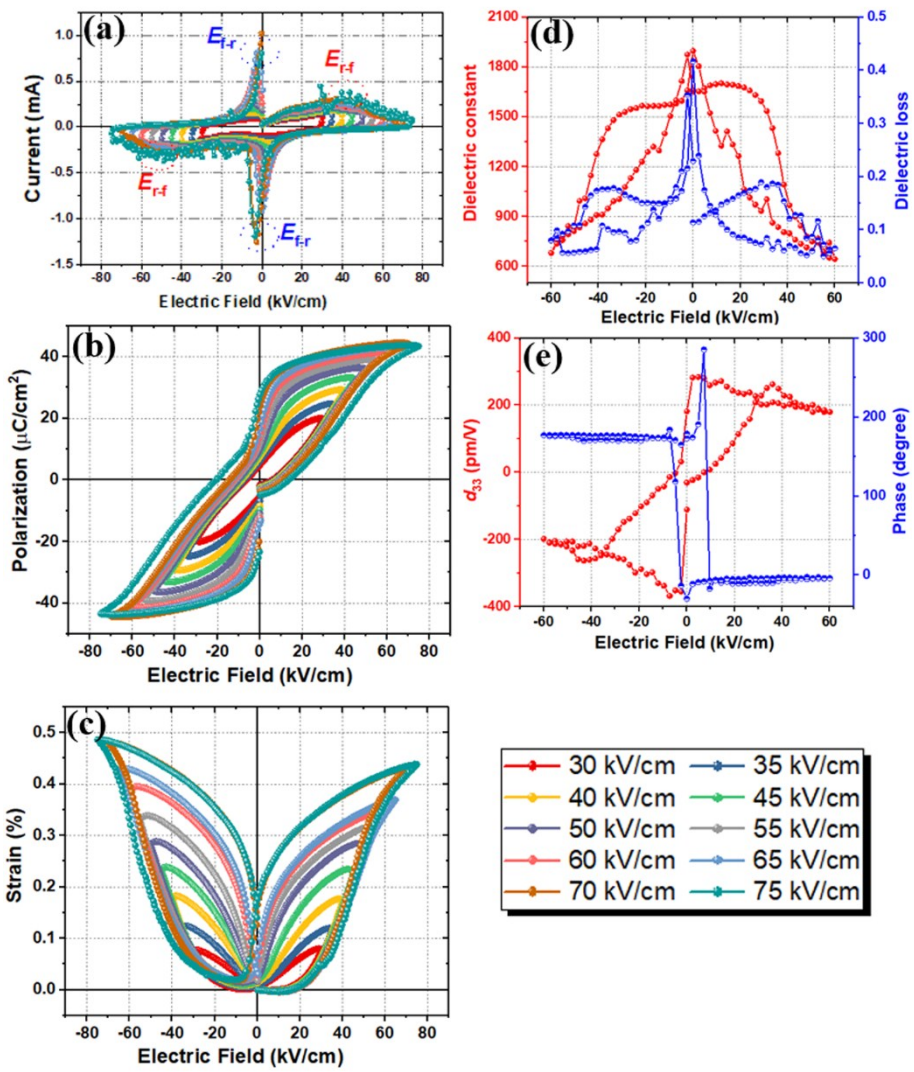

Figure S4. Electric field-dependent (a) current-field curves, (b) polarization hysteresis loops, (c) bipolar strain curves, (d) dielectric constant and loss, and (e) piezoelectric strain coefficient and phase curves for the oriented ceramics.

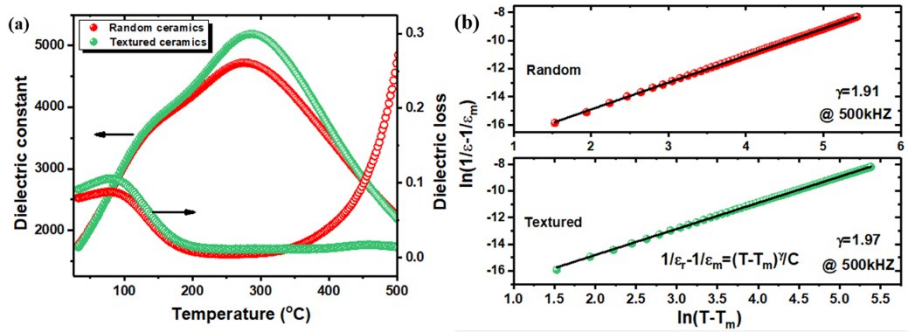

Figure S5. (a) Dielectric constant and loss as a function of temperature, and (b) the diffuseness parameter γ for the poled random and textured ceramics. The *insert* is the modified Curie-Weiss equation.

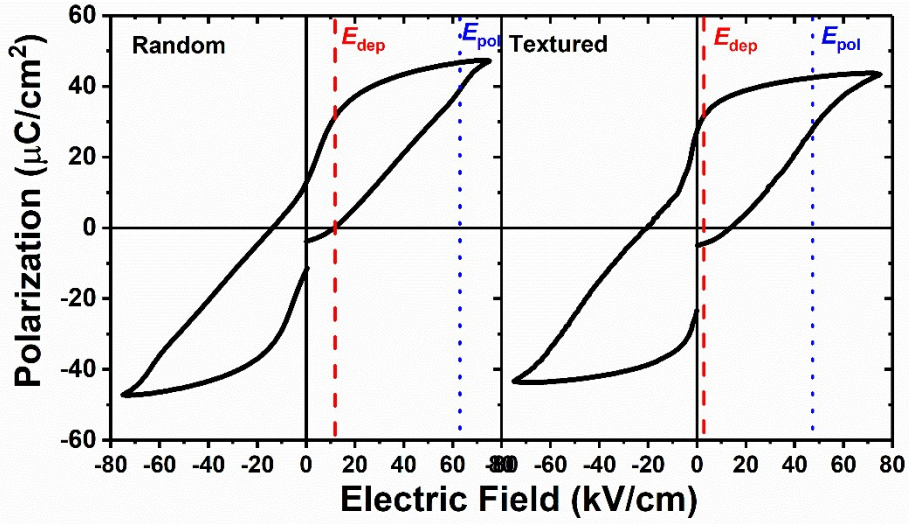

Figure S6. Polarization hysteresis loops of random and textured ceramics measured at 75kV/cm. The inflection point during uphill and downhill cycle corresponds to the E_{dep} and E_{pol}, respectively.

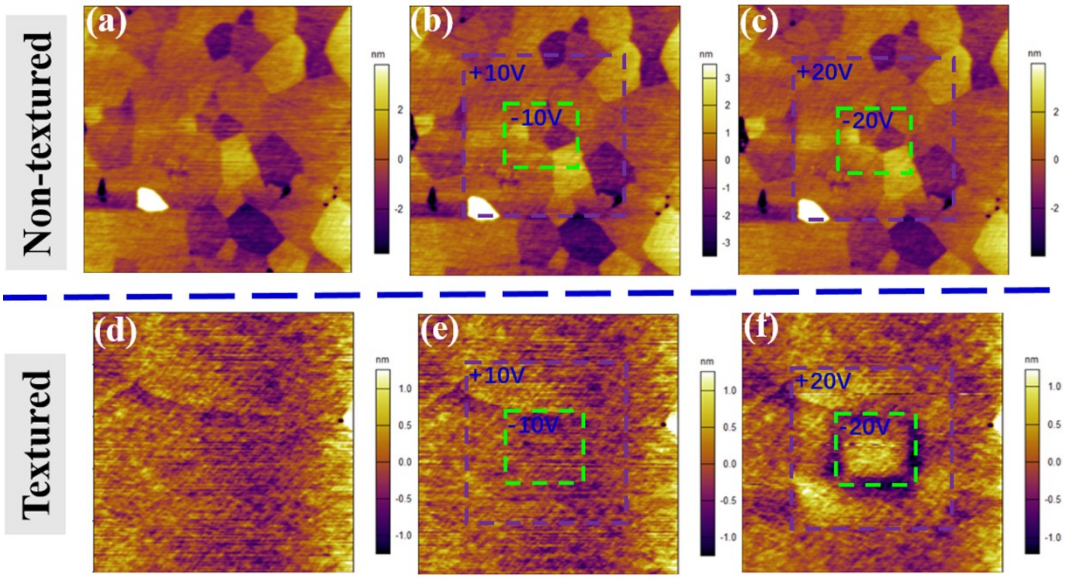

Figure S7. Morphology of randomly oriented and oriented BNT-BT-NN ceramics.

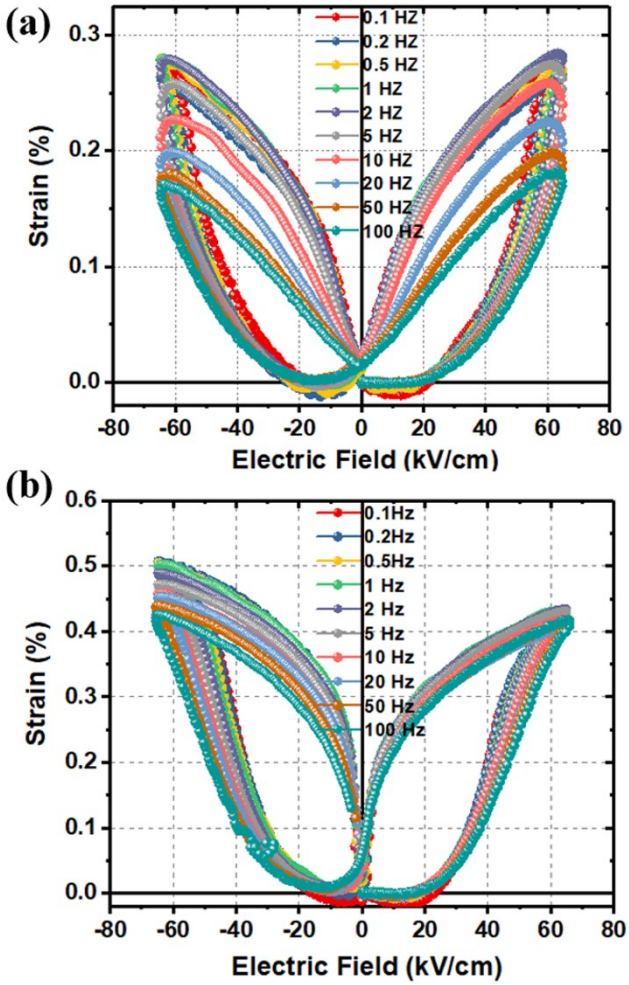

Figure S8. Frequency-dependent bipolar strain curves for (a) random and (b) textured BNT-BT-NN ceramics.

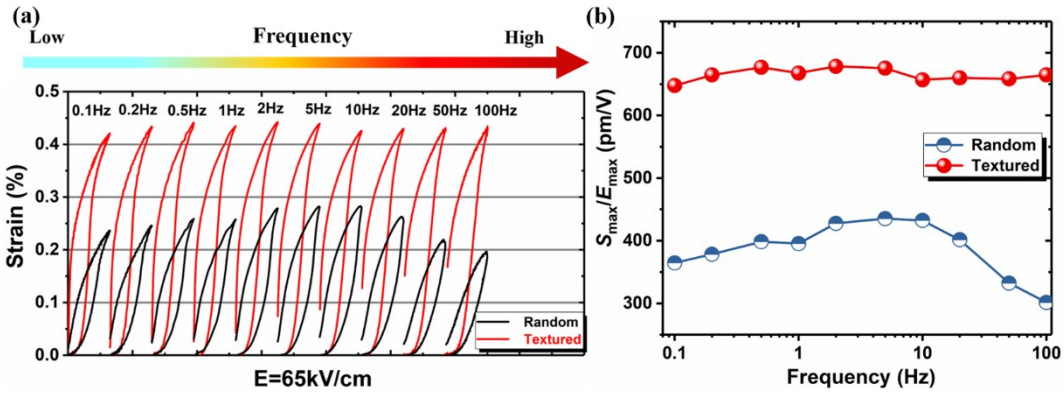

Figure S9. (a)Field-induced unipolar strain of the non-textured and textured BNT-BT-NN ceramics under different measuring frequency, and (b) the change of normalized S_{max}/E_{max} as a function of measuring frequency.

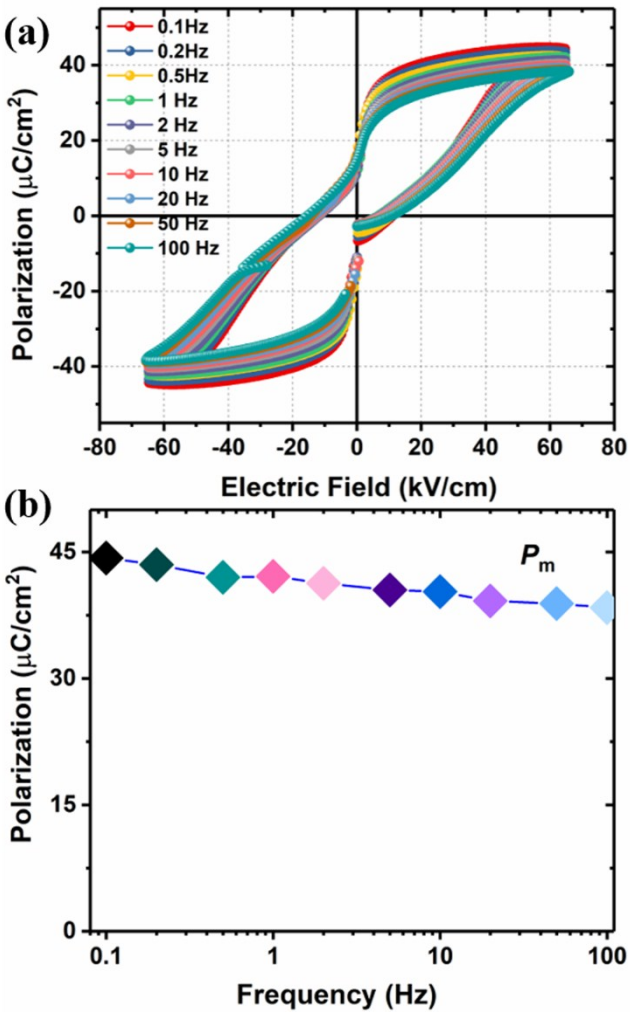

Figure S10. (a) Frequency-dependent polarization hysteresis loops, and (b) the variation in P_m with respect to frequency for the textured BNT-BT-NN sample.

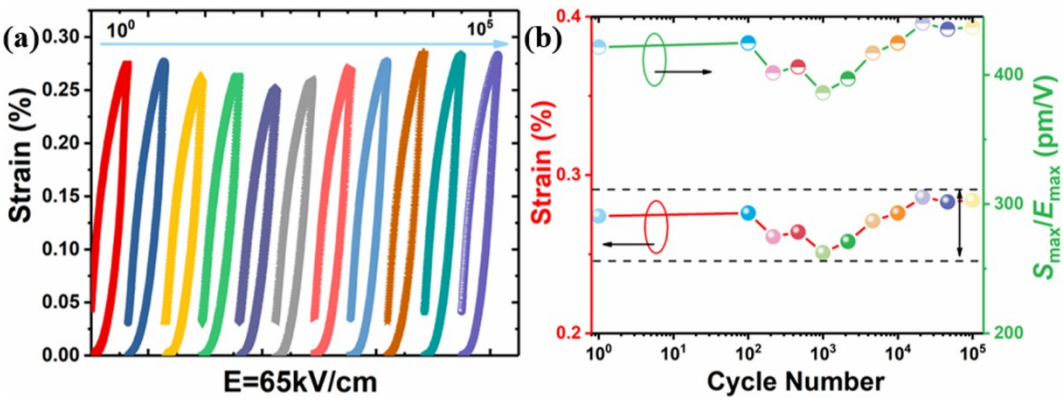

Figure S11. (a) Unipolar strain curves with respect to cycle numbers, and (b) the change of unipolar strain and normalized S_{max}/E_{max} as a function of cycle numbers for the random BNT-BT-NN ceramics.

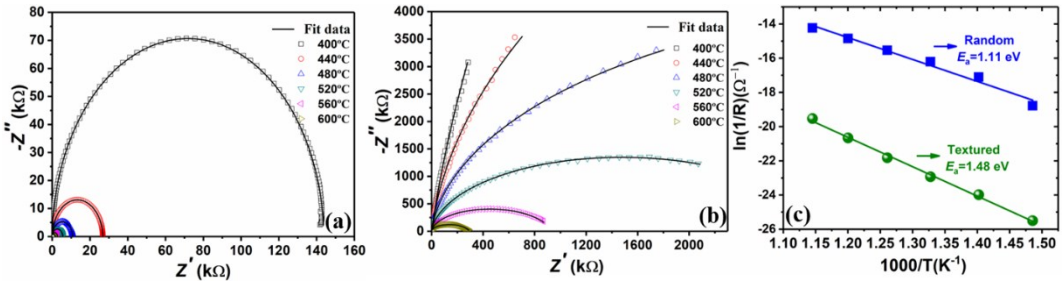

Figure S12. Complex impedance spectra of (a) random and (b) textured BNT-BT-NN ceramics measured at 400°C-600°C from 100Hz to 10MHz. (c) The change of bulk resistance with inverse of temperature. The activation energy E_a was determined using the Arrhenius law: $\sigma=\sigma_0 \exp(-E_a/kT)$, where σ_0 represents the pre-exponent constant and k is Boltzmann constant.